J. Phase Equilib. Diffus. (2018) 39:549–561
https://doi.org/10.1007/s11669-018-0635-2

Phase Equilibria of the Ti-Al-Nb System at 1000, 1100 and 1150 °C

Lin Li[1] · Libin Liu[1,2] · Ligang Zhang[1] · Lijun Zeng[1] · Yun Zhao[1] · Weimin Bai[1] · Yurong Jiang[1]

Submitted: 30 March 2018 / in revised form: 3 May 2018 / Published online: 17 May 2018

Abstract 1000, 1100 and 1150 °C isothermal sections of the Ti-Al-Nb system were studied using x-ray diffraction, scanning electron microscopy and electron probe microanalysis. A small island-like region of single β_0 is present at 1000, but absent at 1100 and 1150 °C. γ_1 is not a stable phase at 1000 and 1150 °C. Three three-phase fields ($\alpha_2 + \beta_0 + \sigma$, $\beta_0 + \sigma + \gamma$ and $\alpha_2 + \beta_0 + \gamma$) are identified in the 1000 °C isothermal section (30-60 at.% Ti content). The 1100 °C isothermal section is firstly studied completely. It includes six three-phase and thirteen two-phase fields. Two three-phase fields $\beta + \alpha_2 + \gamma$ and $\beta + \sigma + \gamma$ are identified in the isothermal section (30-60 at.% Ti content) at 1150 °C. These data are helpful to the fabrication of the TiAl and Ti_2AlNb intermetallics.

Keywords intermetallics · microstructure · phase diagram · TiAl alloy

Dedicate to the celebration of Prof. Zhanpeng Jin's 80th birthday.

This invited article is part of a special issue of the *Journal of Phase Equilibria and Diffusion* in honor of Prof. Zhanpeng Jin's 80th birthday. The special issue was organized by Prof. Ji-Cheng (JC) Zhao, The Ohio State University; Dr. Qing Chen, Thermo-Calc Software AB; and Prof. Yong Du, Central South University.

✉ Libin Liu
PDC@CSU.EDU.CN; lbliu@csu.edu.cn

✉ Ligang Zhang
ligangzhang@csu.edu.cn

[1] School of Materials Science and Engineering, Central South University, Changsha 410083, People's Republic of China

[2] State Key Laboratory of Powder Metallurgy, Central South University, Changsha 410083, People's Republic of China

1 Introduction

Ti-Al intermetallic phases have excellent mechanical properties and good oxidation resistance up to 700 °C.[1–8] The alloying element Nb is used to enhance their oxidation resistance, hot formability and creep resistance.[9–12] The ternary Ti-Al-Nb system also contains many intermetallics which have a potential for producing alloys with various mechanical properties.[4] Recently, advanced materials based on the Ti-Al-Nb alloys that can be used at temperatures above 800 °C have been investigated.[13] The alloys normally show multiple-phase microstructures consisting of γ-TiAl, α_2-Ti_3Al, O-Ti_2NbAl, σ-Nb_2Al and β-ordered solid solution, i.e. β_0.[4,14–16]

The fundamental knowledge, e.g. the information about phase equilibria in the Ti-Al-Nb related systems is indispensible for the design and fabrication of these intermallic based alloys.[17] Phase diagrams of the three constituent binary systems, i.e., Ti-Al,[18–20] Ti-Nb,[21,22] and Al-Nb,[23] have been well investigated and assessed.

Hellwig [24] studied partial isothermal section at 1000 and 1200 °C. Leonard[25] studied partial isothermal section at 1100 °C. Chen[26] and Ding[27] studied the isothermal section at 1000, 1150 and 1400 °C by diffusion couples. Jewett[28] commented Chen's work,[26] and their results about γ_1 phase are different. There are also some literature regarding the calculation of the Ti-Al-Nb ternary phase diagram using thermodynamic methods.[20,23,29–32] Witusiewicz[23] and Cupid[29] independently optimized the Ti-Al-Nb ternary phase diagram using the CALPHAD (Calculation of Phase Diagrams) method in 2009. Witusiewicz re-evaluated the Al-Ti[19] and Al-Nb[23] binary systems. Crystal structures of phases in the Ti-Al-Nb ternary system are summarized in Table 1.

Table 1 The phase designations most often used in literature for the Al–Nb–Ti system along with crystal structure data[23]

Phase (designation)	Pearson symbol	Space group	Strukturbericht designation	Prototype
(Al)(αAl), fcc_A1	cF4	Fm-3m	A1	Cu
α, (αTi), hcp_A3	hp2	$P6_3/mmc$	A3	Mg
α_2, Ti_3Al	hP8	$P6_3/mmc$	$D0_{19}$	Ni_3Sn
β, (βTi), bcc_A2	cI2	Im-3m	A2	W
β_0, bcc_B2	cI2	Pm-3m	B2	CsCl
γ, γTiAl, TiAl	tP4	P4/mmm	$L1_0$	AuCu
δ, Nb3Al	cP8	Pm-3n	A15	$C_{r3}Si$
ε, $(Ti_{1-x}Nb_x)Al_3$, $TiAl_3$(h), $NbAl_3$	tI8	I4/mmm	$D0_{22}$	$TiAl_3$(h)
ε(l), $TiAl_3$(l)	tI32	I4/mmm	…	$TiAl_3$(l)
ζ, $Ti_{2+x}Al_{5-x}$	tP28	P4/mmm	…	Ti_2Al_5
η, $TiAl_2$	tI24	$I4_1/amd$	…	$HfGa_2$
σ, Nb_2Al	tP30	$P4_2/mnm$	$D8_b$	σCrFe
Ti_3Al_5	tP32	P4/mbm	…	Ti_3Al_5
O_1, O, O_1(h), Ti_2NbAl	oC16	Cmcm	…	NaHg
O_2, O_2(r), Ti_2NbAl	oC16	Cmcm	…	NaHg
τ, Ti_4NbAl_3	hP6	$P6_3/mmc$	$B8_2$	Ni_2In
γ_1-$Ti_4Nb_3Al_9$	tP16	P4/mmm	…	γ_1-$Ti_4Nb_3Al_9$

Table 2 Equilibrium compositions at 1000 °C measured with EPMA method

Number	Alloy, at.%			Phase equilibrium	Phase composition, at.%					
	Al	Ti	Nb	Phase 1/Phase 2/Phase 3	Phase 1		Phase 2		Phase 3	
					Al	Ti	Al	Ti	Al	Ti
#A1	23.7	32.5	43.8	β/δ/σ	24.8	58.7	21.0	31.2	29.5	29.8
#A2	26.8	45.8	27.4	α_2/β/σ	25.0	59.1	22.5	49.3	30.1	33.3
#A3	34.3	50.0	15.7	α_2/β_0/σ	33.1	55.3	34.1	50.9	33.2	36.7
#A4	38.9	51.5	9.6	α_2/β_0/γ	34.4	56.2	34.5	53.0	44.1	46.6
#A5	18.0	22.0	60.0	β/δ	7.0	29.1	18.3	21.9		
#A6	16.8	16.4	66.8	β/δ	5.7	21.4	18.2	17.5		
#A7	13.0	16.0	71.0	β/δ	4.7	17.6	18.1	13.8		
#A8	21.1	6.1	72.8	δ/σ	21.3	6.4	30.3	6.5		
#A9	42.5	53.1	4.4	α_2/γ	35.6	60.1	45.9	49.5		
#A10	36.5	33.5	30.0	γ/σ	45.3	40.9	33.9	30.7		
#A11	46.0	35.0	19.0	γ/σ	47.1	37.8	34.1	27.3		
#A12	50.0	28.0	22.0	γ/σ	51.9	25.3	35.9	13.9		
#A13	40.7	17.6	41.7	γ/σ	51.4	23.1	35.5	13.4		
#A14	63.0	11.5	25.5	γ/σ/ε	54.2	22.0	37.1	12.9	72.9	3.4
#A15	58.2	10.8	31.0	γ/σ/ε	54.6	21.7	36.0	11.6	73.1	2.7
#A16	63.0	20.0	17.0	ε/γ	72.5	6.1	55.3	30.4		
#A17	65.2	28.7	6.1	γ/η/ε	57.3	37.0	65.2	31.4	73.1	14.9
#A18	68.5	26.3	5.2	η/ε	65.6	32.8	74.3	14.7		
#A19	37.8	43.5	18.7	β_0/γ/σ	34.4	50.5	44.0	44.6	33.7	36.3
#A20	33.5	55	11.5	α_2/β_0	32.6	57.6	33.5	53.0		

The Nb concentration in each phase can be calculated as 100—(Al concentrationin at.% + Ti concentration in at.%)

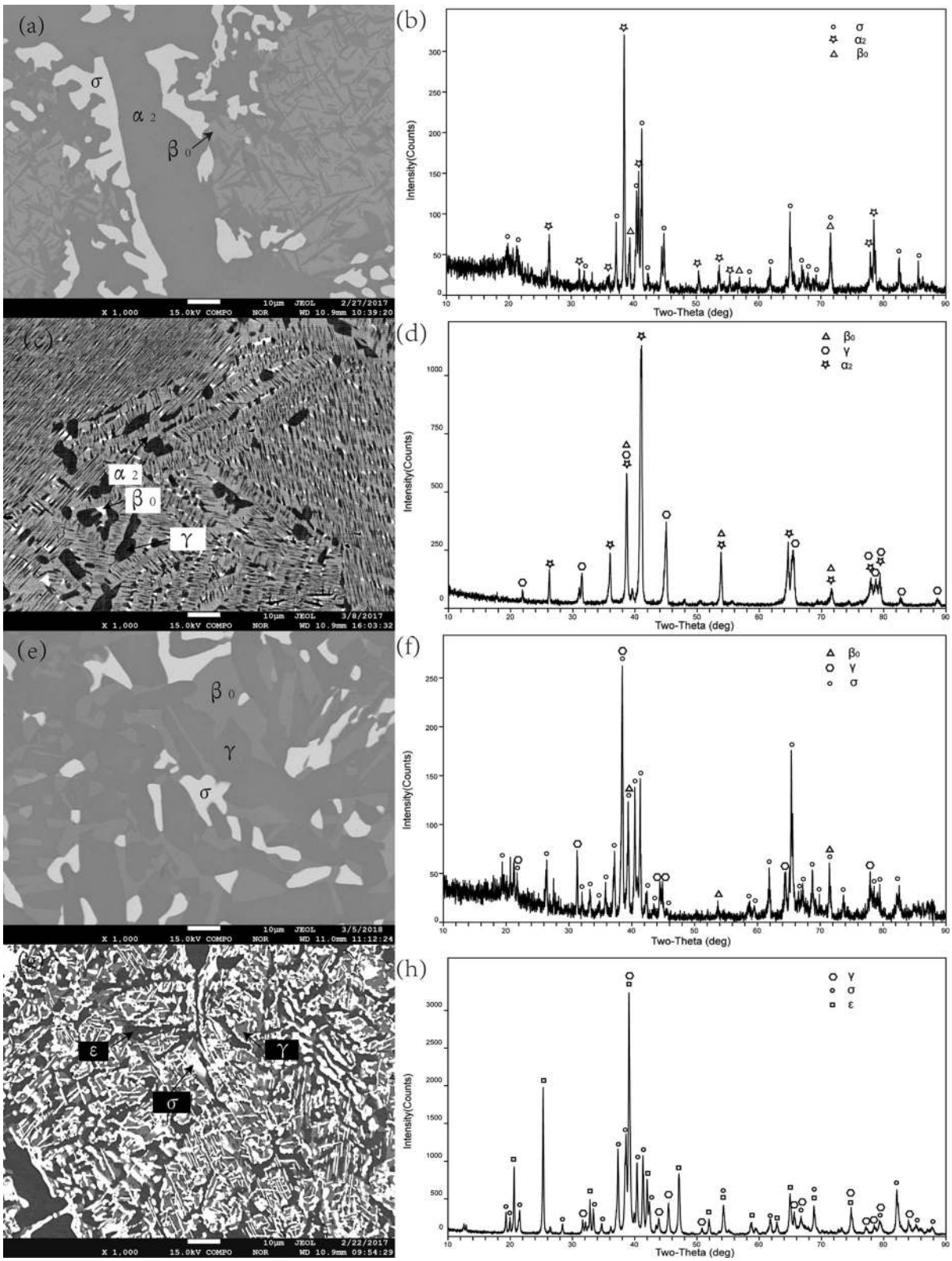

Fig. 1 EPMA images and XRD results of typical alloys after annealing at 1000 °C, which contain three phases after quenching: (a) the microstructure of alloy #A3, (b) the XRD result of alloy #A3, (c) the microstructure of alloy #A4, (d) the XRD result of alloy #A4, (e) the microstructure of alloy #A19, (f) the XRD result of alloy #A19, (g) the microstructure of alloy #A15 and (h) the XRD result ofalloy #A15

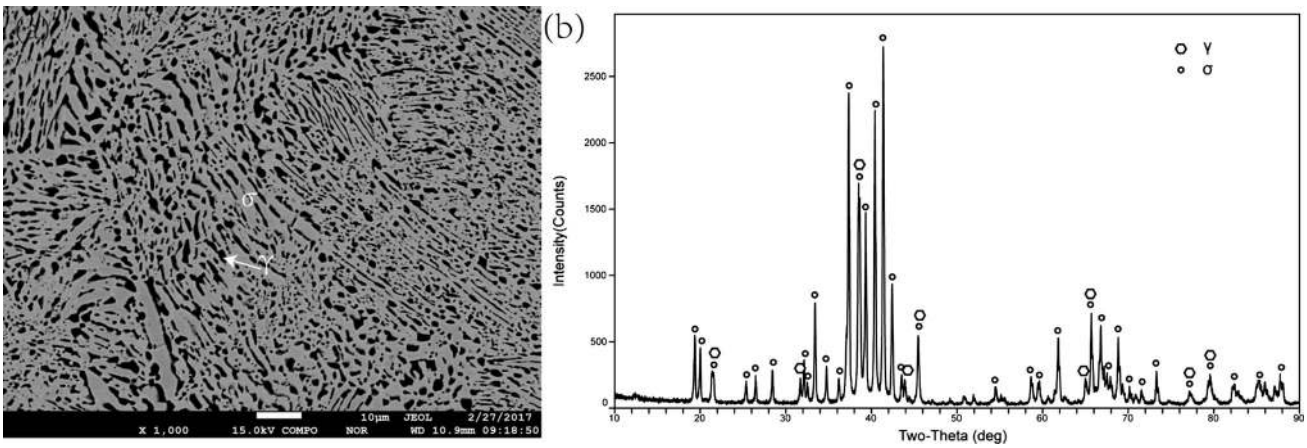

Fig. 2 EPMA images and XRD results of typical alloys after annealing at 1000 °C, which contain two phases after quenching: (a) the microstructure of alloy #A13 and (b) the XRD result of alloy #A13

However, there are many differences between the experimental results. For example, Chen[26] and Ding[27] found that there is a γ_1 phase existing in this ternary system. However, this phase has not been found by Hellwig. Hellwig found that a small island-like region of single β_0 is a stable phase at 1000 °C, however it was not found by Chen[26] and Ding.[27] For this reason, the phase equilibria at 1000, 1100 and 1150 °C in the Ti-Al-Nb system was re-investigated using SEM (Scanning Electron Microscope), EPMA (Electron Probe Microanalysis) and XRD (x-ray diffraction) in this work.

2 Experimental

More than 35 samples have been prepared to measure the isothermal section of Ti-Al-Nb ternary system at 1000, 1100 and 1150 °C. The starting materials Ti, Al and Nb (purity of all 99.99%) supplied by China Jinyu Materials Technology Co., Ltd. were used to prepare the experimental alloys. The weight of each sample was limited to about 6 g. Predetermined amount of each raw material was weighted by analytical balance, and followed by arc-melting on a water-cooled copper crucible under argon atmosphere. The hot/liquid titanium has been used as oxygen getter. To ensure a good homogeneity of the samples, each obtained button was turned over and re-melted at least three times. The weight losses did not exceed 1%. The obtained button alloys were sealed in a silica capsule back-filled with high purity argon, and then annealed at 1000 °C for 1440 h, 1100 °C for 1080 h or 1150 °C for 360 h in diffusion furnace. After annealing, the alloys were quenched into ice water.

The annealed specimens were polished and their microstructure were investigated using electron probe microanalysis (EPMA) (JEOL JXA-8530F). Standard deviations of the measured concentration is ± 0.5 at.%. The total mass of Ti, Al and Nb in each phase is in the range of 97-103%. No silicon was found in the samples, so the effect of reactions between the samples and silica capsules could be neglected. XRD was also performed for phase identification in some selected annealed alloys using a Cu Kα radiation on a Rigaku D-max/2500 x-ray diffractometer operated at 40 kV and 200 mA. Phase identification and calculation of the lattice parameters of each phase were carried out using the Jade 6.0 program.

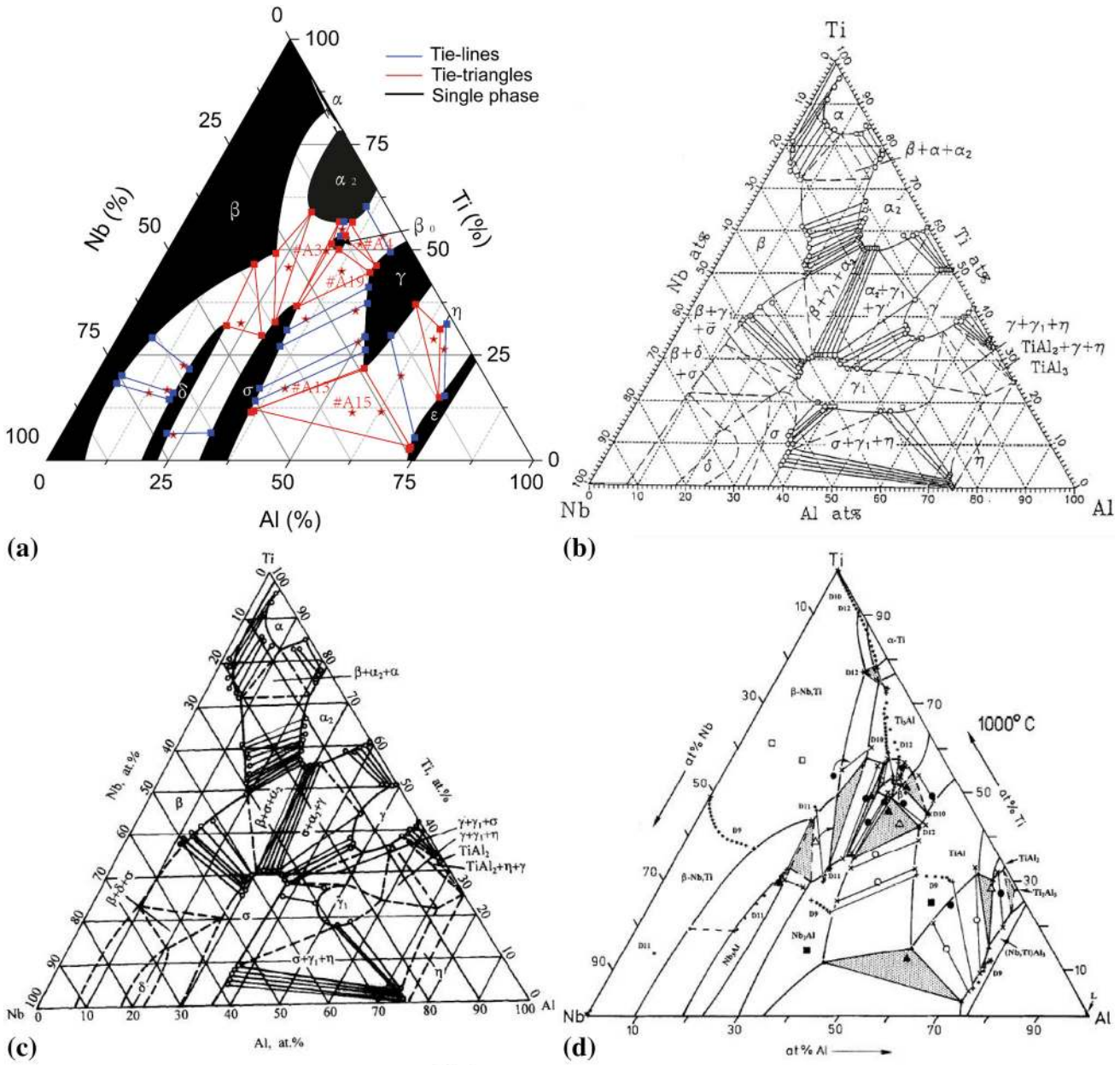

Fig. 3 The 1000 °C isothermal section of the Ti-Al-Nb system: (a) the tie-lines, the tie-triangles and the measured 1000 °C isothermal section in the present work, (b) the experimental results from Chen's work,[26] (c) the experimental results from Ding's work[27] and (d) the experimental results from Hellwig's work[24]

3 Results and Discussion

3.1 Isothermal Section at 1000 °C

The nominal chemical compositions of the alloys and the measured chemical compositions of individual phases by EPMA at 1000 °C samples are given in Table 2.

Figure 1(a) shows the microstructure of alloy #A3, which contains α_2 (gray phase), β_0 (light gray phase) and σ (bright phase) based on the XRD result (see Fig. 1b). Whereas, the alloy #A4 is located in the $\alpha_2 + \beta_0 + \gamma$ three-phase area (see Fig. 1c and d). Figure 1(e) illustrates the EPMA micrograph of the alloy #A19, which featured a three-phase $\sigma + \gamma + \beta_0$ that agrees with the XRD result shown in Fig. 1(f). Figure 1(g) shows the microstructure of alloy #A15, which contains ε (dark gray phase), γ (light gray phase) and σ (bright phase).

Figure 2(a, b) shows the EPMA micrograph and XRD result of the alloy #A13, which featured a two-phase equilibrium $\sigma + \gamma$.

Table 3 Equilibrium compositions at 1100 °C measured with EPMA method

Number	Alloy, at.%			Phase equilibrium	Phase composition, at.%					
	Al	Ti	Nb	Phase 1/Phase 2/Phase 3	Phase 1		Phase 2		Phase 3	
					Al	Ti	Al	Ti	Al	Ti
#B1	23.7	32.5	43.8	β/δ/σ	18.4	43.5	21.0	28.8	28.9	27.3
#B2	26.6	48.6	24.8	α_2/β/σ	25.7	58.7	24.3	48.5	30.1	32.3
#B3	34.3	51.2	14.5	α_2/σ	34.3	52.7	33.5	35.1		
#B4	39.1	43.2	17.7	α_2/γ/σ	37.4	48.5	45.2	40.0	34.5	30.6
#B5	42.5	53.1	4.4	α_2/γ	36.2	59.9	47.1	48.2		
#B6	18.0	22.0	60.0	β/δ	9.7	29.9	18.5	21.8		
#B7	16.8	16.4	66.8	β/δ	7.9	18.8	18.2	15.1		
#B8	11.3	16.4	72.3	β/δ	6.3	16.2	17.7	13.4		
#B9	24.0	16.0	60.0	δ/σ	20.9	17.0	30.0	15.7		
#B10	46.0	35.0	19.0	γ/σ	46.4	37.1	35.0	27.5		
#B11	50.0	28.0	22.0	γ/σ	50.2	28.9	35.9	18.8		
#B12	49.7	24.1	26.2	γ/σ	52.0	24.9	36.9	15.1		
#B13	42.0	14.5	43.5	γ/σ	52.9	23.1	37.3	13.3		
#B14	58.2	10.8	31.0	γ/σ/ε	53.4	23.9	38.2	12.1	72.2	4.0
#B15	50.0	6.3	43.7	σ/ε	36.2	8.9	70.3	2.7		
#B16	63.0	20.0	17.0	γ/ε	55.7	28.7	72.1	7.1		
#B17	70.2	24.4	5.4	η/ε	65.7	32.3	73.8	16.7		

The Nb concentration in each phase can be calculated as 100—(Al concentrationin at.% + Ti concentration in at.%)

Based on the tie-lines and tie-triangles identified by the present work, the isothermal section at 1000 °C was thus constructed as illustrated in Fig. 3(a).

Figure 3(b, c and d) shows the experimental results of the 1000 °C isothermal section by Chen,[26] Ding[27] and Hellwig[24]. Chen[26] and Ding[27] reported the existence of γ_1 phase, while Hellwig[24] didn't found it. The present result is consistent with Hellwig's result,[24] and a two-phase σ + γ field in this area. In the Ti 30-60 at.% region, Chen[26] and Ding[27] reported two three-phase fields ($\beta + \gamma_1 + \alpha_2$ and $\alpha_2 + \gamma_1 + \gamma$) and one two-phase field ($\alpha_2 + \gamma_1$). However in this composition range Hellwig[24] reported three three-phase fields ($\alpha_2 + \beta_0 + \sigma$, $\beta_0 + \sigma + \gamma$ and $\alpha_2 + \beta_0 + \gamma$), three two-phase fields ($\alpha_2 + \beta_0$, $\beta_0 + \sigma$ and $\beta_0 + \gamma$) and one single-phase field (β_0). The phase relationship of the present work is consistent with Hellwig's work.[24]

3.2 Isothermal Section at 1100 °C

The nominal compositions of the alloys investigated in this work and chemical compositions of the individual phases at 1100 °C samples as determined by EPMA are given in Table 3.

Figure 4(a) shows the three-phase microstructure of $\beta + \sigma + \delta$ for alloy #B1, and the XRD result is showed in Fig. 4(b). The existence of the three-phase field $\beta + \alpha_2 + \sigma$ and its location are also established based on the SEM, EPMA and XRD data of alloy #B2 in Fig. 4(c, d).

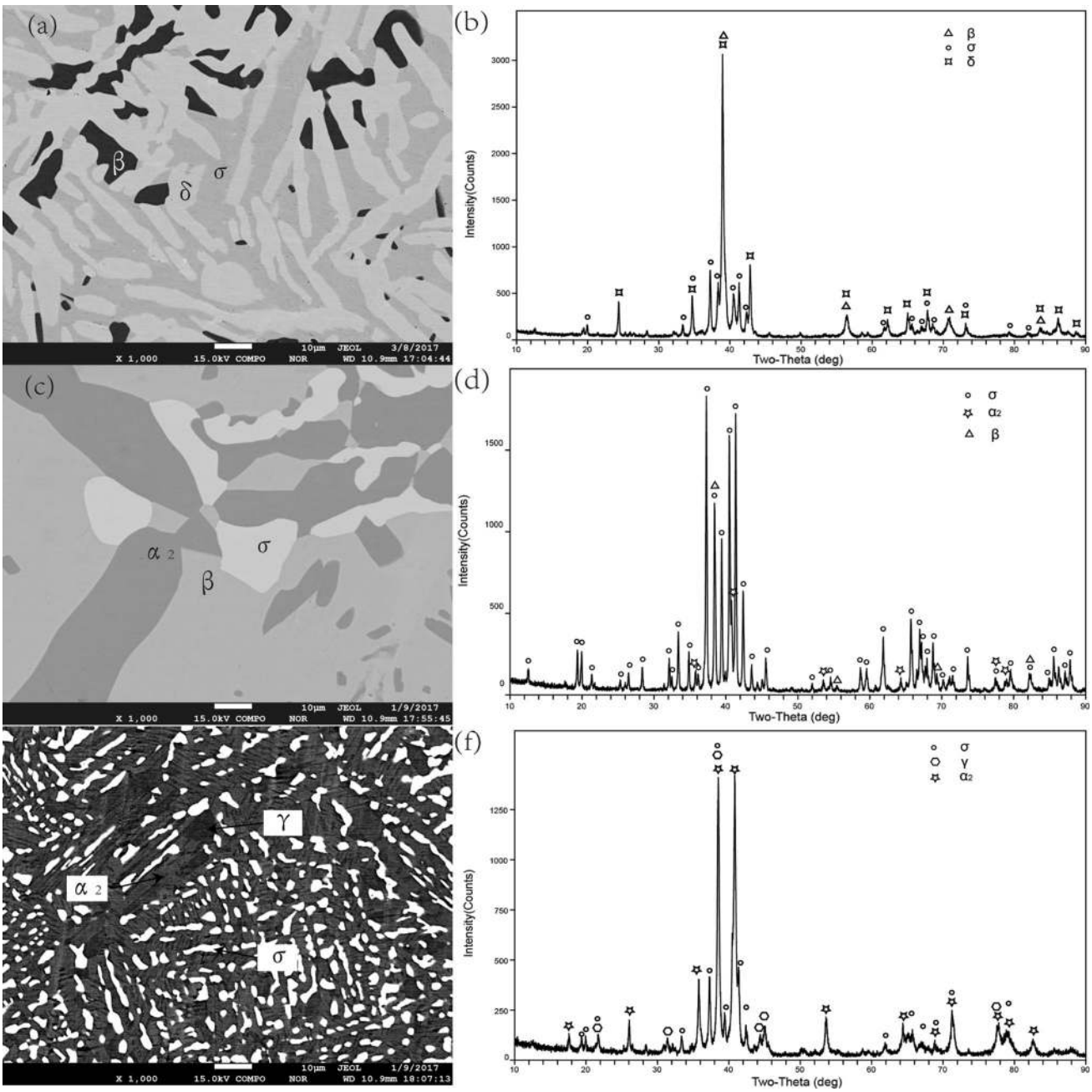

Fig. 4 EPMA images and XRD results of typical alloys after annealing at 1100 °C, which contain three phases after quenching: (a) the microstructure of alloy #B1, (b) the XRD result of alloy #B1, (c) the microstructure of alloy #B2, (d) the XRD result of alloy #B2, (e) the microstructure of alloy #B4 and (f) the XRD result of alloy #B4

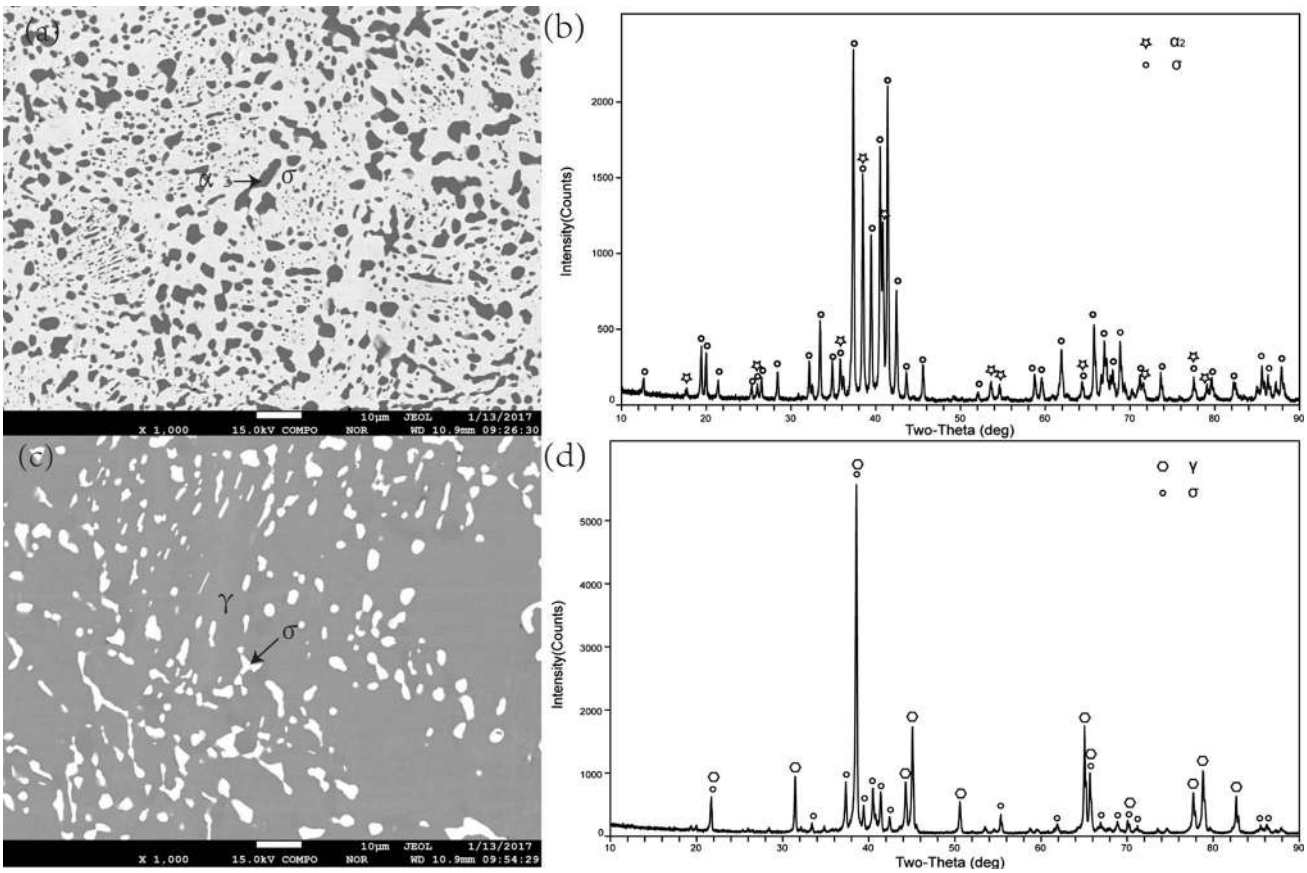

Fig. 5 EPMA images and XRD results of typical alloys, which contain two phases after quenching: (a) the microstructure of alloy #B3, (b) the XRD result of alloy #B3, (c) the microstructure of alloy #B10 and (d) the XRD result of alloy #B10

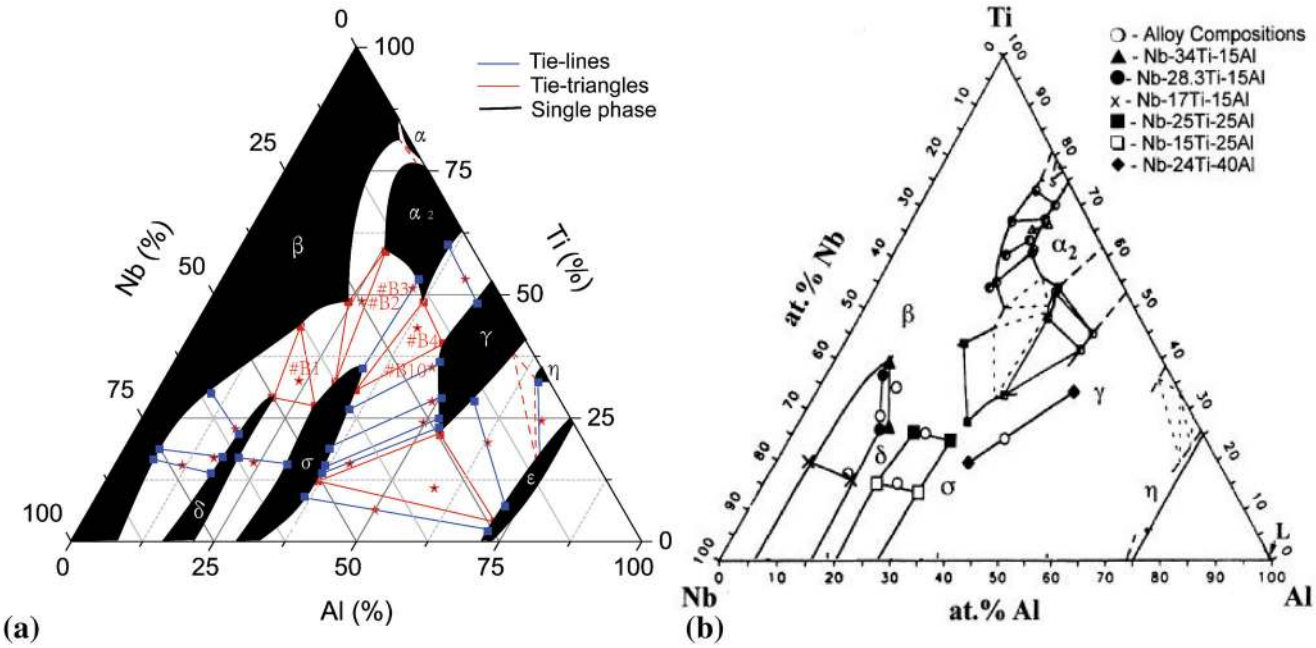

Fig. 6 The 1100 °C isothermal section of phase diagrams: (a) the tie-lines, the tie-triangles and the 1100 °C isothermal section of phase diagram constructed by the present work and (b) Experimental isotherm of Leonard's work[25] accomplished with experimental data of Kattner[33]

Table 4 Equilibrium compositions at 1150 °C measured with EPMA method

Number	Alloy (at.%)			Phase equilibrium	Phase composition (at.%)					
	Al	Ti	Nb	Phase 1/Phase 2/Phase 3	Phase 1		Phase 2		Phase 3	
					Al	Ti	Al	Ti	Al	Ti
#C1	23.7	32.5	43.8	β/δ/σ	18.7	39.5	20.9	25.8	29.1	24.5
#C2	39.1	43.2	17.7	β/γ/σ	36.1	45.7	44.8	40.6	35.1	32.9
#C3	38.9	51.5	9.6	α_2/β/γ	37.5	53.1	36.0	52.6	44.7	46.1
#C4	42.5	53.1	4.4	α_2/γ	37.8	57.9	45.6	50.2		
#C5	13.0	23.0	63.0	β/δ	8.6	23.1	18.6	17.3		
#C6	13.0	16.0	71.0	β/δ	6.7	16.5	18.0	13.2		
#C7	21.1	6.1	72.8	δ/σ	20.0	5.2	29.9	4.9		
#C8	46.0	35.0	19.0	γ/σ	47.3	35.8	35.2	26.7		
#C9	50.0	28.0	22.0	γ/σ	50.6	28.2	36.6	19.2		
#C10	42.0	14.5	43.5	γ/σ	53.2	22.6	37.8	13.3		
#C11	63.5	13.0	23.5	γ/ε	54.8	21.1	72.0	4.5		
#C12	63.0	20.0	17.0	γ/ε	56.9	27.7	72.1	7.4		
#C13	68.5	26.3	5.2	γ/η/ε	62.4	41.4	64.8	40.5	72.7	18.6
#C14	31.9	58.1	10.0	α_2/β	31.5	60.0	32.3	56.2		
#C15	37.9	47.7	14.4	β/γ	35.8	49.5	44.3	43.7		
#C16	34.6	42.5	22.9	β/σ	34.7	47.4	33.9	34.2		
#C17	57.2	11.3	31.5	γ/σ/ε	54.1	21.0	37.7	12.5	72.0	4.4

The Nb concentration in each phase can be calculated as 100—(Al concentrationin at.% + Ti concentration in at.%)

Based on the XRD and EPMA results (see Fig. 4e and f), the $\sigma + \gamma + \alpha_2$ equilibrium is observed.

Figure 5(a) shows the two-phase $\alpha_2 + \sigma$ microstructure for alloy #B3 that agrees with the XRD result presented in Fig. 5(b). Figure 5(c) illustrates the $\gamma + \sigma$ microstructure for alloy #B10, and the XRD result is shown in Fig. 5(d).

Figure 6(a) shows the tie-lines and tie-triangles for isothermal section at 1100 °C identified by the present work. Six three-phase and thirteen two-phase fields exit in the isothermal section (0-70 at.% Al content). Figure 6(b) shows the experimental isotherm of Leonard's work[25] accomplished by experimental data of Kattner.[33]

3.3 Isothermal Section at 1150 °C

Phases occurring in various samples annealed at 1150 °C are summarized in Table 4. Figure 7(a) exhibits microstructure image of alloy #C1, where three phases can be observed, including dark β, dark gray σ and white δ that agrees with the XRD results shown in Fig. 7(b). Two three-phase $\beta + \sigma + \gamma$ and $\alpha_2 + \beta + \gamma$ equilibria are found in the alloy #C2 and alloy #C3 (Fig. 7c and e) and the XRD patterns of them are shown in Fig. 7(d, f).

Two-phase equilibrium of $\sigma + \gamma$ was found in the alloy #C10 (Fig. 8a) and XRD spectrum is shown in Fig. 8(b).

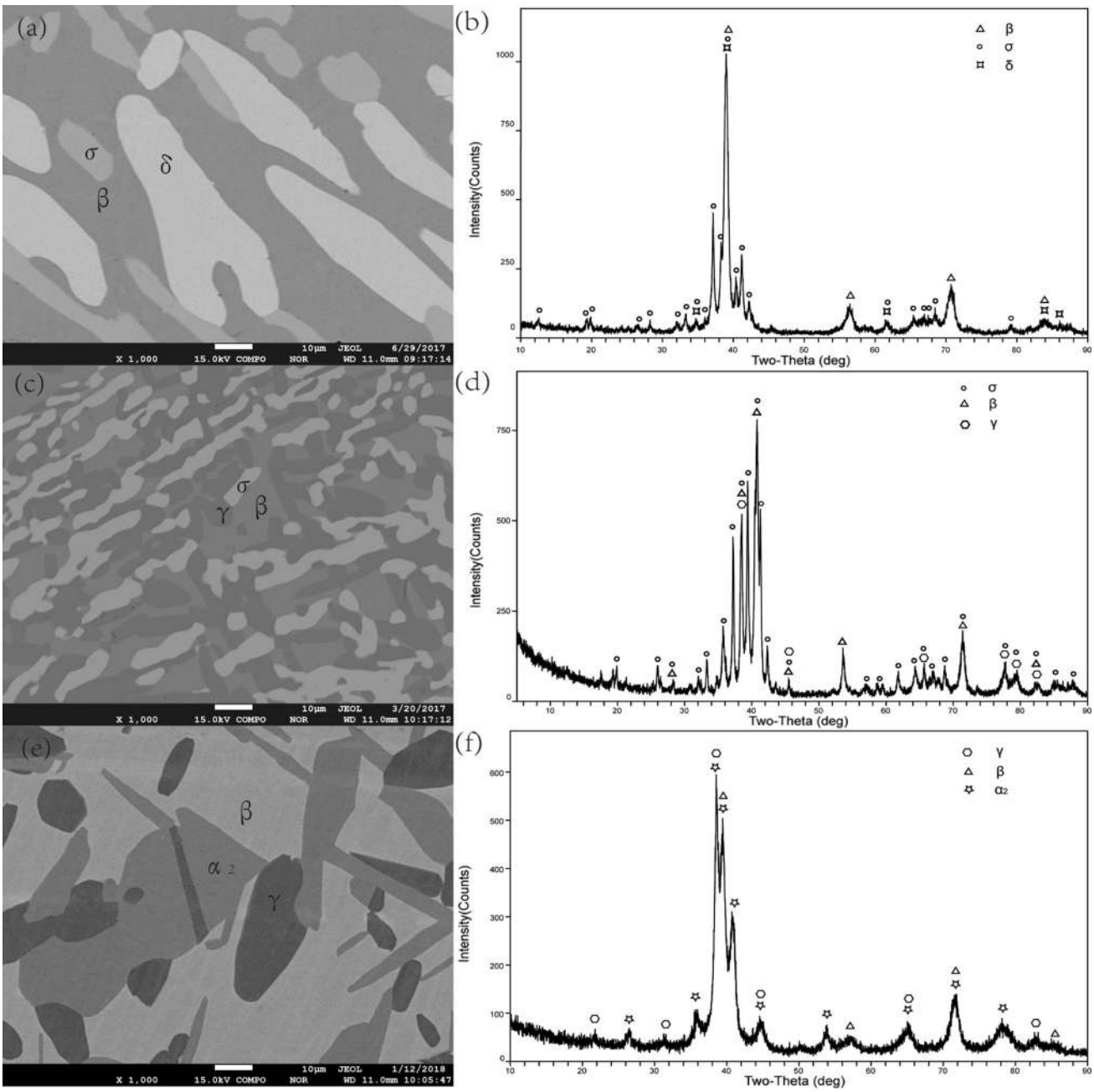

Fig. 7 EPMA images and XRD results of typical alloys, which contain three phases after quenching: (a) the microstructure of alloy #C1, (b) the XRD result of alloy #C1, (c) the microstructure of alloy #C2, (d) the XRD result of alloy #C2, (e) the microstructure of alloy #C3 and (f) the XRD result of alloy #C3

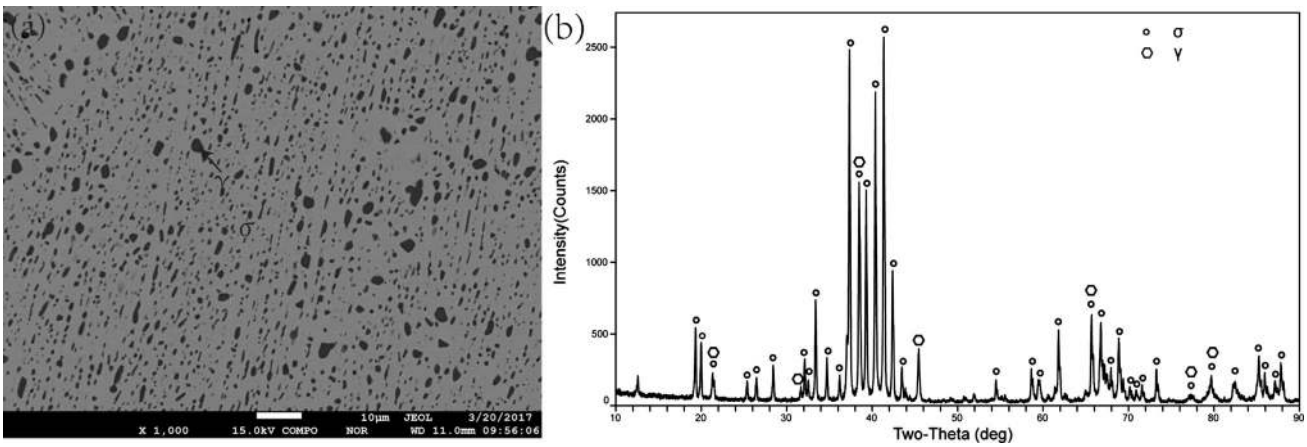

Fig. 8 EPMA images and XRD results of typical alloys, which contains three phases after quenching: (a) the microstructure of alloy #C10 and (b) the XRD result of alloy #C10

The identified tie-lines, tie-triangles, and the 1150 °C isothermal section of phase diagram constructed in the present work are illustrated in Fig. 9(a). Figure 9(b and c) shows the experimental results of the 1150 °C isothermal section from Chen's work[26] and Ding's work.[27] Figure 9(d) shows the experimental result of the 1200 °C isothermal section from Zhao's work.[34] The data in the previous work of isothermal section at 1150 °C is limited. Chen's[26] and Ding's[27] experimental results support existence of γ_1 phase, while according to the present work exits one two-phase field ($\sigma + \gamma$) in this area. Two three-phase fields ($\beta + \alpha_2 + \gamma$, $\beta + \sigma + \gamma$) are identified in Ti 30-60 at.% in the present work. The three-phase field $\beta + \delta + \sigma$ is also identified in the present work. Phase relationships between Zhao's work[34] and present wok is quite similar.

4 Conclusions

The isothermal sections of the Ti-Al-Nb ternary system at 1000, 1100 and 1150 °C were determined using electron probe microanalysis and x-ray diffraction.

1. A small island-like region of single β_0 present at 1000 °C, but absent at 1100 and 1150 °C. γ_1 is not a stable phase at 1000 and 1150 °C.

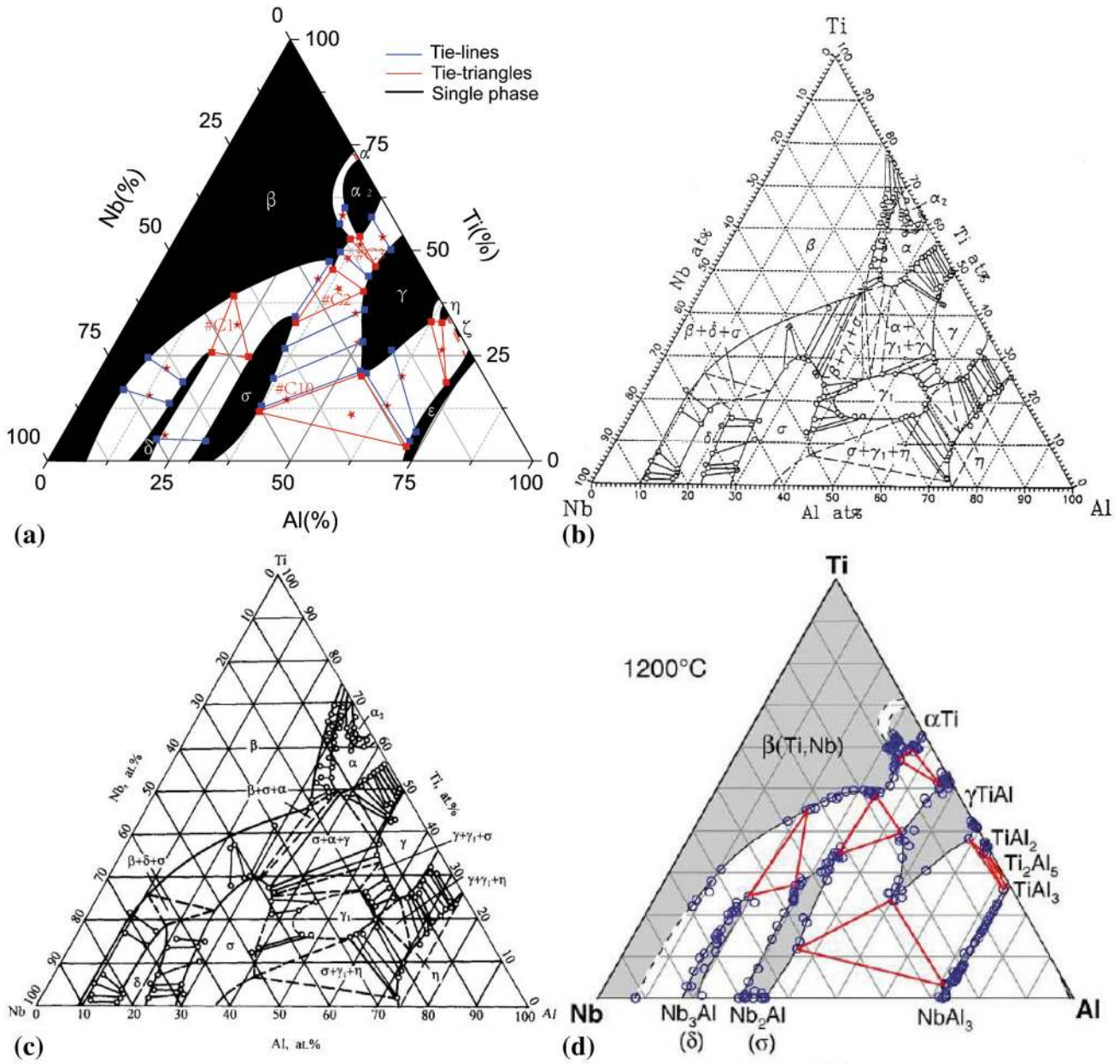

Fig. 9 The of phase diagrams: (a) the tie-lines, the tie-trianges and the 1150 °C isothermal section of phase diagram constructed by the present work, (b) the experimental 1150 °C isothermal section from Chen's work,[26] (c) the experimental 1150 °C isothermal section from Ding's work[27] and (d) the experimental 1200 °C isothermal section from Zhao's work[34]

2. Three three-phase fields ($\alpha_2 + \beta_0 + \sigma$, $\beta_0 + \sigma + \gamma$ and $\alpha_2 + \beta_0 + \gamma$) are identified in the 1000 °C isothermal section (30-60 at.% Ti content).
3. The 1100 °C isothermal section is firstly studied completely. Six three-phase and thirteen two-phase fields exit in the isothermal section (0-70 at.% Al content).
4. Two three-phase fields ($\beta + \alpha_2 + \gamma$, $\beta + \sigma + \gamma$) are identified in the isothermal section (30-60 at.% Ti content) at 1150 °C.

Acknowledgments The work was financially supported by National Key Technologies R&D Program of China (Grant No. 2016YFB0701301), National Natural Science Foundation of China (Grant Numbers 51671218, 51501229). National Key Basic Research Program of China (973 Program) (Grant No. 2014CB644000).

References

1. S.H. Kayani and N.-K. Park, Effect of Cr and Nb on the Phase Transformation and Pore Formation of Ti-Al base alloys, *J. Alloys Compd.*, 2017, **708**, p 308-315

2. Y. Shida and H. Anada, Oxidation Behavior of Binary Ti-Al Alloys in High Temperature Air Environment, *Mater. Trans. JIM*, 1993, **34**(3), p 236-242
3. T.M. Pollock, Alloy Design for Aircraft Engines, *Nat. Mater.*, 2016, **15**(8), p 809-815
4. B.J. de Aragão and F. Ebrahimi, High Temperature Deformation of Nb-Ti-Al Alloys with σ+γ Microstructure, *Mater. Sci. Eng. A*, 1996, **208**(1), p 37-46
5. G. Chen, Y. Peng, G. Zheng, Z. Qi, M. Wang, H. Yu, C. Dong, and C.T. Liu, Polysynthetic Twinned TiAl Single Crystals for High-Temperature Applications, *Nat. Mater.*, 2016, **15**(8), p 876-881
6. R. Chen, D. Zheng, J. Guo, T. Ma, H. Ding, Y. Su, and H. Fu, A Novel Method for Grain Refinement and Microstructure Modification in TiAl Alloy by Ultrasonic Vibration, *Mater. Sci. Eng. A*, 2016, **653**, p 23-26
7. S. Valkov, P. Petrov, R. Lazarova, R. Bezdushnyi, and D. Dechev, Formation and Characterization of Al-Ti-Nb Alloys by Electron-Beam Surface Alloying, *Appl. Surf. Sci.*, 2016, **389**, p 768-774
8. M. Yamaguchi, H. Inui, and K. Ito, High-Temperature Structural Intermetallics, *Acta Mater.*, 2000, **48**(1), p 307-322
9. C. Kenel and C. Leinenbach, Influence of Nb and Mo on Microstructure Formation of Rapidly Solidified Ternary Ti-Al-(Nb, Mo) Alloys, *Intermetallics*, 2016, **69**(Supplement C), p 82-89
10. H. Clemens, W. Wallgram, S. Kremmer, V. Güther, A. Otto, and A. Bartels, Design of Novel β-Solidifying TiAl Alloys with Adjustable β/B2-Phase Fraction and Excellent Hot-Workability, *Adv. Eng. Mater.*, 2008, **10**(8), p 707-713
11. Y.W. Kim, Ordered Intermetallic Alloys, Part III: Gamma Titanium Aluminides, *JOM*, 1994, **46**(7), p 30-39
12. O. Shuleshova, D. Holland-Moritz, W. Löser, A. Voss, H. Hartmann, U. Hecht, V.T. Witusiewicz, D.M. Herlach, and B. Büchner, In Situ Observations of Solidification Processes in γ-TiAl Alloys by Synchrotron Radiation, *Acta Mater.*, 2010, **58**(7), p 2408-2418
13. D. Hoelzer and F. Ebrahimi, Phase Stability of sigma+beta Microstructures in the Ternary Nb-Ti-Al System, *MRS Proc.*, 1990, **194**, p 393
14. H. Clemens and S. Mayer, Design, Processing, Microstructure, Properties, and Applications of Advanced Intermetallic TiAl Alloys, *Adv. Eng. Mater.*, 2013, **15**(4), p 191-215
15. D.M. Dimiduk, Gamma Titanium Aluminide Alloys—An Assessment Within the Competition of Aerospace Structural Materials, *Mater. Sci. Eng. A*, 1999, **263**(2), p 281-288
16. X. Wu, Review of Alloy and Process Development of TiAl Alloys, *Intermetallics*, 2006, **14**(10–11), p 1114-1122
17. Y. Liu, L.F. Chen, H.P. Tang, C.T. Liu, B. Liu, and B.Y. Huang, Design of Powder Metallurgy Titanium Alloys and Composites, *Mater. Sci. Eng. A*, 2006, **418**(1–2), p 25-35
18. Y. Fujita, H. Mitsui, K. Ishikawa, R. Kainuma, and K. Ishida, Phase Equilibria in the Ti-Al Binary System, *Acta Mater.*, 2000, **48**, p 3113-3123
19. V.T. Witusiewicz, A.A. Bondar, U. Hecht, S. Rex, and T.Y. Velikanova, The Al-B-Nb-Ti System : III. Thermodynamic Re-evaluation of the Constituent Binary System Al-Ti, *J. Alloys Compd.*, 2008, **465**(1–2), p 64-77
20. U.R. Kattner, J.C. Lin, and Y.A. Chang, Thermodynamic Assessment and Calculation of the Ti-Al System, *Metall. Trans. A*, 1992, **23**(8), p 2081-2090
21. K.C.H. Kumar, P. Wollants, and L. Delaey, Thermodynamic Calculation of Nb-Ti-V Phase Diagram, *CALPHAD*, 1994, **18**(1), p 71-79
22. V.T. Witusiewicz, A.A. Bondar, U. Hecht, S. Rex, and T.Y. Velikanova, The Al-B-Nb-Ti System: II. Thermodynamic Description of the Constituent Ternary System B-Nb-Ti, *J. Alloys Compd.*, 2008, **456**(1), p 143-150
23. V.T. Witusiewicz, A.A. Bondar, U. Hecht, and T.Y. Velikanova, The Al-B-Nb-Ti system: IV. Experimental Study and Thermodynamic re-evaluation of the Binary Al-Nb and Ternary Al-Nb-Ti Systems, *J. Alloys Compd.*, 2008, **472**(1), p 133-161
24. A. Hellwig, M. Palm, and G. Inden, Phase Equilibria in the Al-Nb-Ti System at hIgh Temperatures, *Intermetallics*, 1998, **6**(2), p 79-94
25. K.J. Leonard, J.C. Mishurda, and V.K. Vasudevan, Phase Equilibria at 1100 C in the Nb-Ti-Al System, *Mater. Sci. Eng. A*, 2002, **s329–331**(01), p 282-288
26. G.L. Chen, X.T. Wang, K.Q. Ni, S.M. Hao, J.X. Cao, J.J. Ding, and X. Zhang, Investigation on the 1000, 1150 and 1400 °C Isothermal Section of the Ti-Al-Nb System, *Intermetallics*, 1996, **4**(1), p 13-22
27. J.J. Ding and S.M. Hao, Reply to the "Comment on 'Investigation on the 1000, 1150 and 1400 °C Isothermal Section of the Ti-Al-Nb System'"—Part II. MODIFICATION of 1000 and 1150 °C Isothermal Sections of the Ti-Al-Nb System, *Intermetallics*, 1998, **6**(4), p 329-334
28. T.J. Jewett, Comment on 'Investigation on the 1000, 1150 and 1400 °C iso th ermal sect ion of the Ti-Al-Nb syst em', *Intermetallics*, 1997, **5**(2), p 157-159
29. D.M. Cupid, O. Fabrichnaya, O. Rios, F. Ebrahimi, and H.J. Seifert, Thermodynamic r e-assessment of the Ti-Al-Nb sys tem, *Int. J. Mater. Res.*, 2009, **100**(2), p 218-233
30. C. Servant and I. Ansara, Thermodynamic assessm ent of the Al-Nb-Ti syste m, *Ber. Bunsenges. Phys. Chem.*, 1998, **102**(9), p 1189-1205
31. C. Servant and I. Ansara, Thermodynamic Modelling of the Order–Disorder Transformation of the Orthorhombic Phase of the Al-Nb-Ti System, *CALPHAD*, 2001, **25**(4), p 509-525
32. Z. Zhu, Y. Du, L. Zhang, H. Chen, H. Xu, C. Tang, Z. Zhu, Y. Du, and C. Tang, Experimental Identification of the Degenerated Equilibrium and Thermodynamic Modeling in the Al-Nb System, *J. Alloys Compd.*, 2008, **460**(1), p 632-638
33. U.R. Kattner and W.J. Boettinger, Thermodynamic Calculation of the Ternary Ti-Al-Nb System, *Mater. Sci. Eng. A*, 1992, **152**(1), p 9-17
34. J.C. Zhao, Reliability of the Diffusion-Multiple Approach for Phase Diagram Mapping, *J. Mater. Sci.*, 2004, **39**(12), p 3913-3925